

# Customizable Coherent Servo Demodulation for Disk Drives

Daniel Abramovitch  
Hewlett-Packard Laboratories  
Storage Technologies Department  
1501 Page Mill Road, M/S 4U-12  
Palo Alto, CA 94304  
Phone: (650) 857-3806  
E-mail: danny@hpl.hp.com

## Abstract

This paper describes a servo demodulator which provides dramatically improved performance over the currently used servo demodulation methods for disk drives. The demodulation algorithm proposed here makes better use of knowledge about the readback signal coming from the disk to provide better noise immunity and more immunity to other non-idealities in the magnetic head response. The net result is a demodulated Position Error Signal (PES) which has a much cleaner response.

## 1 Introduction

This paper describes an algorithm for servo demodulation in a disk drive that can significantly lower the Position Sensing Noise (PSN) that gets into the servo channel of a disk drive. It does this by mixing the servo burst signal with an idealized version of the dibit response and integrating over a finite, integral number of periods of the waveform. This differs from demodulation schemes which use rectifiers (almost all disk drives). It is also different from the amplitude modulated (AM) signal demodulation problem found in communications systems. Typically, the latter are trying to extract a continuous signal rather than a burst of information that yields a single number. A servo demodulator is after a single number from a burst of information. This also differs from a matched filter demodulator because this formulation allows potentially undesirable portions of the “noise free signal” to be excluded from the demodulation process.

The main idea is to use the frequency selectivity of an algorithm similar to that used in measuring frequency responses, the swept-sine demodulation algorithm[1], to get far better noise immunity than standard disk drive servo demodulators. A logical question to ask is why this has not been done by others. The reasons are most likely that:

- such an algorithm is difficult to implement in analog hardware and
- there has not been a perceived need for such noise immunity in the disk drive servo problem in the past.

However, recent results obtained using the PES Pareto Method[2, 3, 4, 5] have shown that as disk drive servo bandwidths are pushed higher and higher, the amplification by the servo loop of Position Sensing Noise causes major problems. Thus, any method that can reduce the Position Sensing Noise *before* it gets into the servo loop should be quite helpful in allowing the designer to increase the servo bandwidth. Furthermore, the same level of digital hardware that is currently used in modern PRML recording channels should be more than enough to implement this scheme in real time.

## 2 Background

Demodulation is the process for extracting a signal that has been modulated onto a carrier signal. This is one of the fundamental features of any communication or data storage system. In general, demodulation can be done coherently (also called synchronously) or non-coherently.

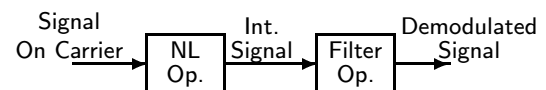


Figure 1: Non-Coherent Demodulation

Non-coherent demodulation (Fig. 1) involves passing the modulated signal through some sort of memoryless nonlinear operator. Furthermore, the nonlinear operator used is one of even order, that is it produces the same sign on the output independently of the sign of the input. This nonlinear operator has the effect (among others) of splitting the signal energy into bands among the multiple

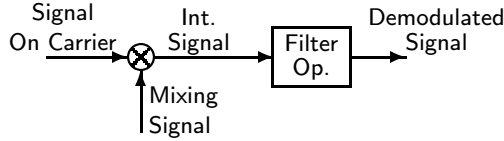


Figure 2: Coherent Demodulation

harmonics of the carrier signal. The filter operation then selects one or some of these harmonic bands – very often the zeroth (0th) harmonic or baseband – and discards the others. If the baseband harmonic is chosen, the signal has effectively been demodulated.

Coherent demodulation (Fig. 2) has a similar goal, but the initial operation is different. Rather than passing the modulated signal through a nonlinear element, the modulated signal is mixed with (multiplied by) another signal. This mixing signal bears a frequency and phase relationship with the carrier, although determination of this relationship might be part of the demodulation problem. However, because there is a relationship between the mixing signal and the carrier signal, this is referred to as coherent demodulation.

The mixed signal also contains various harmonics of the two input signals. In particular, if the mixing signal contains the fundamental frequency of the carrier, then one of the harmonics generated will be the baseband or zeroth (0th) harmonic. As with the non-coherent demodulation, if the filter operation selects the baseband portion, then the signal is demodulated.

As both coherent and non-coherent demodulation are attempting to do the same essential function, one might wonder what the relative merits of each scheme are. In the case of non-coherent demodulation, the advantage is often one of simplicity. Several simple circuits can serve as the nonlinear operator (such as a half or full wave rectifier) and no synchronization with any mixing signal is required.

On the other hand, coherent demodulation often offers improved signal to noise properties. This is due to several factors. First of all, the simple circuits used in non-coherent demodulation are non-ideal and will often distort and add noise to the modulated signal. Second, the generated mixing signal can be free of the noise that is corrupting the modulated signal. (The mixing signal may have some noise of its own, but this is typically significantly lower in level than that of the modulated signal. Furthermore, specific mixing signals can be used that allow the demodulator to mask off a large portion of the input spectrum and with it a large amount of noise and other non-idealities in the signal.)

The cost of this lowered noise level is that the circuit complexity needed to generate the mixing signal is often significantly greater than that needed in non-coherent demodulation. Typically, this requires at least one oscilla-

tor circuit (which is active) rather than simply a passive circuit (such as the rectifier often used in non-coherent demodulation). Furthermore, the mixing signal must be consistently synchronized with the modulated signal, otherwise the phase shift between the two signals requires that both the magnitude and phase of the signal be demodulated. This adds considerable complexity to the system.

Thus, the choice between coherent and non-coherent demodulation has been one of noise immunity versus simplicity. In particular, in the disk drive servo channel non-coherent demodulation has been used predominantly (with a few exceptions that will be discussed below). Until recently, the signal to noise ratio provided by non-coherent demodulation has been considered sufficient for the track densities of disk drives. Hence, drive manufacturers opted for the simpler, cheaper circuits. However, as the push for greater track density intensifies, the noise immunity of the servo demodulation scheme will become a larger issue. Furthermore, many of the general ideas of coherent demodulation have been adopted into the data channels of disk drives, due to the increased use of Partial Response, Maximum Likelihood (PRML) detection. Thus, coherent demodulation for disk drive servo channels may be an idea whose time has come.

## 2.1 Generation of a Position Error Signal from Dibit Fields

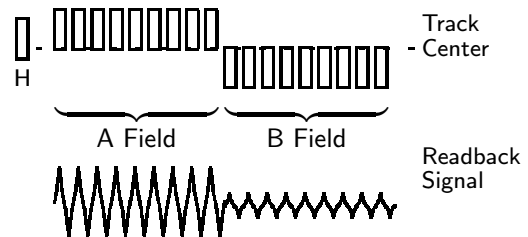


Figure 3: Burst patterns and the resulting readback signals when head is above the track center. The magnetic readback head (transducer) is denoted by the rectangle with the H inside. The vertical position of the rectangle symbolizes the radial position of the readback head. The waveforms at the bottom are the resulting readback signals. Note that the readback signal is multiplexed in time so that the signal obtained from the A Field is processed separately from the signal obtained from the B Field.

The process of creating a position error signal from amplitude encoded signals on a disk drive may be described as follows. Patterns of alternating magnetic polarity are written on the disk surface with a particular frequency. When the magnetic readback head passes over the burst pattern, it reads back a signal that is periodic (in the ideal case) for the length of the burst. The amplitude of that signal (in the ideal case) is proportional to how much

of the read head is directly over the burst pattern at the time the signal is produced.

To compose a Position Error Signal (PES), two patterns, offset by one track width in the radial direction of the disk and put down sequentially in the down track direction of the disk, are used (Fig. 3). By offsetting these signals, the difference between the amplitude demodulated from the first field (A) and the second field (B), can yield a measure of the radial position of the readback head relative to the disk. Typical disk drives today may have servo patterns on the disk which include 2, 4 or even 6 bursts of position information for a given track. For simplicity of explanation, this paper will discuss only the 2 burst pattern. However, the algorithm applies equally well to all of these cases.

## 2.2 Disk Drive Servo Demodulators

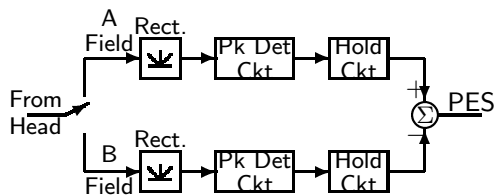


Figure 4: Peak Detection Servo Demodulator

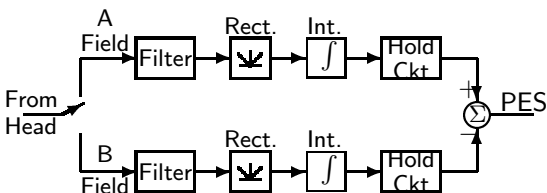


Figure 5: A Rectify and Integrate (commonly called Area Detection) Servo Demodulator with Optional Filtering

In a typical disk drive, the servo demodulation is done non-coherently. Referring back to Figure 1, the nonlinear operation is accomplished with a rectifier. This is typically a full wave rectifier which computes the absolute value of a signal.

The rectifier produces a signal with a large baseband component. (For example, if a sine wave with an amplitude of  $X$  is fed into a full wave rectifier, the output  $y(t)$  will have a Fourier series expansion with the baseband term,  $A_0 = \frac{4X}{\pi}$ , which retains over half of the peak to peak amplitude ( $= 2X$ ) of the original signal.) By processing the rectified signal, the non-coherent demodulator can extract a signal that is related to the original signal's amplitude. This allows amplitude modulated position information to be extracted from the modulated signal. For the vast majority of disk drive servo channels, the recti-

fied signal is processed in one of two ways. One method is called Peak Detection (Fig. 4) (sometimes referred to as “envelope detection”). With peak detection, a circuit is used which detects and holds the peak amplitude value of the rectified signal. The other common method is to integrate the rectified signal. This integration computes the area of the rectified signal and thus the method is often called area detection. Furthermore, filtering may optionally be added to improve the noise immunity of the area detection demodulator (Fig. 5). In the frequency domain, the integration causes all the Fourier components to be averaged to zero except for the baseband term. Broadband noise however, once passed through the rectifier will have a baseband component to it and thus will not average to zero.

The choice between peak detection and area detection is typically based on the types of distortion that the servo designer expects to encounter. Peak detection also typically results in a simpler circuit design. Furthermore, it is less prone to problems such as drop outs and baseline popping (which will be defined in Section 4.3). Furthermore, any distortion which affects the shape of the rectified pulses – but not the peak amplitude – will have no effect on peak detection. By the same token, any sort of distortion that affects the peak signal amplitude – such as as additive white Gaussian noise (AWGN) – will have a serious effect on peak detection.

On the other hand, integration is essentially an averaging operation, so area detection will typically have greater immunity to broadband noise (such as AWGN) than peak detection. Because area detection uses more sophisticated circuitry than peak detection, area detection demodulators are often on separate chips from the read channel (see [6], pages 6:21-6:22). Area detectors are still susceptible to other types of disturbances such as baseline shifts, thermal asperities, signal drop outs, and signal drop ins (which will also be defined in Section 4.3). To deal with some of these issues, manufacturers of these demodulators have begun making hybrid demodulators that contain features from both types of detectors. However, these are still fundamentally non-coherent detectors.

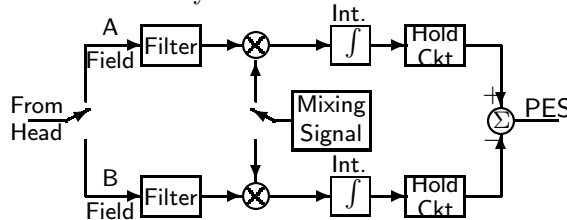


Figure 6: Coherent Servo Demodulation with Optional Filtering

A general block diagram for a coherent demodulator that includes the possibility of pre-filtering the signals is shown in Figure 6. While these diagrams seem

pretty straightforward, coherent servo demodulation for disk drives is far rarer than non-coherent demodulation. Boutaghou et. al. [7] describe a phase encoded position sensing system. In this case the modulated signal is digitized and then mixed with sine and cosine signals separately. Each of these is summed (in a digital approximation to integration) and the ratio of the sums is computed. Finally, the arctangent of the ratio gives the phase encoded position error signal[7]. While this work is well done, it does have the following limitations:

- it is limited to a digital implementation,
- it is for phase encoded position signals only, and
- it mixed with sine and cosine components that contain only the fundamental frequency of the readback signal.

Another all digital coherent demodulation scheme is proposed by Yada and Takeda [8]. They apply a Maximum Likelihood scheme [9] which mixes the sampled modulated signal with a sampled version of the nominal noise free pulse shape. This in fact is what a Maximum Likelihood Detector does. In particular, for the optimum rejection of AWGN, one would want to use the noise free, known amplitude version of the modulated signal to mix. This would, unlike the work of Boutaghou et. al. [7] make use of all the harmonics present in the ideal signal, not simply the first one.

It is worth noting that coherent demodulation has been used in communications system for years. The method involves coherently mixing a square wave with an amplitude encoded signal. This effectively rectifies the signal, but has some improvements in the noise rejection of the signal. One application of this to the disk drive servo demodulation problem is described in Wilson[10]. Wilson describes a method where the dibit signals are synchronously mixed with a square wave of the same frequency as the dibit carrier frequency. The square wave is reconstructed by locking a phase locked oscillator to a field immediately preceding the dibit signals and is thus phase synchronized with them. The net result is that the dibit signal is synchronously rectified before being integrated.

The above method of coherent demodulation as well as the previously described methods of non-coherent demodulation share the same shortfall in that they make very little use of prior knowledge of the dibit signal. It is well known that the optimum solution (at least for minimizing AWGN) is to coherently mix the dibit signal with an idealized (noise free) version of itself. This is essentially what is done in Yada and Takeda[8]. By doing so, they are essentially using what is known as a matched filter and therefore getting a tremendously well matched narrow band filter to shield out additive noise. However, this work only considers the case with two specific restrictions:

- their system is only defined for an all digital implementation and
- they only consider the Maximum Likelihood (matched filter) method which is equivalent to mixing with *all* the harmonics of the nominal noise free position signal.

Note that the coherent demodulation scheme can be implemented for the standard amplitude encoded burst patterns or for the null encoded burst patterns.

### 3 Description of the Algorithm

The method proposed below has several improvements over the aforementioned ones. Like the work by Yada and Takeda [8] and that by Boutaghou et. al. [7], it uses a mixing signal that is composed only of a weighted sum of the harmonics of the dibit carrier frequency to achieve improved filtering of broadband noise. Unlike those methods, this algorithm may be implemented in analog, digital, or hybrid forms, while still maintaining the same essential algorithm. Also, unlike those algorithms, the specific harmonics used in the mixing signal can be adjusted to optimize the immunity to both AWGN and nonlinear effects such as the pulse asymmetry from a magnetoresistive (MR) head.

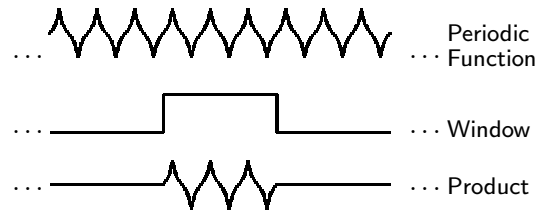


Figure 7: Ideal Dibit Signal can be composed of a periodic signal and a windowing operation.

It turns out that any of the above methods can be examined in the frequency domain. As the ideal dibit pattern (no noise or distortion) produces a periodic signal multiplied times a windowing operation (Fig. 7). One can analyze the periodic function using Fourier series analysis. This states that *any* periodic signal can be decomposed into the sum of the harmonics of the fundamental frequency (the frequency at which the signal repeats itself). Thus a periodic signal,  $m(t)$ , can be decomposed as:

$$m(t) = A_0 + \sum_{n=1}^{\infty} (A_n \cos(n\omega t) + B_n \sin(n\omega t)) \quad (1)$$

where

$$A_n = \frac{1}{\pi} \int_0^{2\pi} m(t) \cos(n\omega t) d(\omega t), \quad (2)$$

$$B_n = \frac{1}{\pi} \int_0^{2\pi} m(t) \sin(n\omega t) d(\omega t), \text{ and} \quad (3)$$

$$A_0 = \frac{1}{\pi} \int_0^{2\pi} m(t)d(\omega t). \quad (4)$$

The core idea of this new method can now be described succinctly. *The demodulating signal that is mixed with the dibit signal is made up of a customizable set of harmonics of the noise free dibit signal.*

By being able to choose *which* harmonics we elect to use, we can optimize the practical performance of the system in the presence of a wide variety of non-idealities which will be discussed in Section 4.3. Furthermore, we will discuss implementation strategies which make it easy for the designer to add or remove harmonics at will.

### 3.1 Mathematical Basis for the Algorithm

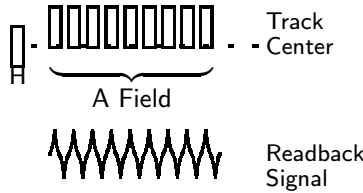


Figure 8: Burst patterns and the resulting readback signal for a single burst.

Consider the readback signal from a single burst field with no noise or distortions as shown in Figure 8. This signal will begin at a zero value, repeat at each new dibit, and terminate at a zero value. The inverse of the period of a dibit,  $T$ , will be the fundamental frequency at which the signal repeats,  $f = \frac{1}{T} = \frac{\omega}{2\pi}$ . In general, there are  $M$  periods of the signal ( $M$  dibits) in the burst. As shown in Figure 7, we can represent the burst as a product of a periodic signal and a window function. Thus, we can analyze the burst by first analyzing the periodic function.

In general, a periodic signal,  $r(t)$ , can be analyzed using Fourier Series analysis, i.e. substituting  $r(t)$  for  $m(t)$  in Equations 1–4. Due to the symmetry properties of this particular signal and the fact that our signal has a zero DC value and is an odd function, it turns out that we can considerably reduce this to

$$r(t) = \sum_{\substack{n=1, \\ n \text{ odd}}}^{\infty} B_n \sin(n\omega t). \quad (5)$$

We will first consider the following signal:

$$r(t) = R_0 \sin \omega t + n(t) \quad (6)$$

where  $n(t)$  is AWGN. We will multiply this by the mixing signal,  $m(t)$ , defined as

$$m(t) = \sin \omega t \quad (7)$$

yielding

$$m(t)r(t) = R_0(\sin \omega t)^2 + (\sin \omega t)n(t). \quad (8)$$

We now integrate this mixed signal for an integral number of periods of the signal, i.e. if  $T = \frac{1}{f}$  is the dibit period where  $f = \frac{\omega}{2\pi}$ , then

$$\frac{1}{MT} \int_0^{MT} m(t)r(t)dt = \frac{R_0}{2} + \frac{1}{MT} \int_0^{MT} (\sin \omega t)n(t)dt. \quad (9)$$

Since  $n(t)$  is a random variable, we cannot integrate the second term directly. However, we can take the expected value. If we assume that  $n(t)$  is a zero mean AWGN, then

$$E \left\{ \frac{1}{MT} \int_0^{MT} (\sin \omega t)n(t)dt \right\} = \frac{1}{MT} \int_0^{MT} (\sin \omega t)E \{n(t)\} dt = 0. \quad (10)$$

Finally,

$$E \left\{ \frac{1}{MT} \int_0^{MT} m(t)r(t)dt \right\} = \frac{R_0}{2}. \quad (11)$$

Thus, this mixing signal and integration scheme demodulates the amplitude of the signal. Now let us consider the more generalized case of a signal

$$r(t) = R_0 (r_1 \sin \omega t + r_3 \sin 3\omega t + r_5 \sin 5\omega t) + n(t) \quad (12)$$

and the mixing signal  $m_n(t) = \sin n\omega t$ , ( $n = 1, 3, 5$ ) which yields through similar operations

$$E \left\{ \frac{1}{MT} \int_0^{MT} m_n(t)r(t)dt \right\} = \frac{R_0 r_n}{2}. \quad (13)$$

(Note that for a square wave demodulator,  $m(t)$  contains an infinite sum of odd harmonics and thus the square wave demodulator can be considered a special case of the new demodulation method. Another important special case is that where  $m(t)$  contains only a single sine wave at the fundamental frequency. We will label this case as *Sine Mixing* in Section 4.)

### 3.2 Purposely Ignoring Particular Harmonics

It should be apparent from this that we can choose to demodulate or ignore *any* individual harmonic. Furthermore, it should be obvious that we can compose a single *custom mixing signal* that contains the harmonics that we wish to demodulate and ignores those that we wish to ignore. In particular, unlike the matched filter approach, we can choose to ignore some harmonics which may contain distortions peculiar to certain classes of disk drives.

However, we are still free to demodulate any harmonics of the signal that increase our signal to noise ratio. This is an extremely useful property in demodulating disk drive servo position from bursts written on the disk.

Two examples are illustrative here. In the first case we consider  $r(t)$  as defined in Equation 12. In this case, choosing

$$m(t) = r_1 \sin \omega t + r_3 \sin 3\omega t + r_5 \sin 5\omega t \quad (14)$$

should maximize the signal to noise ratio. It is equivalent to using a matched filter.

The second example comes from the use of Magneto-Resistive (MR) readback heads as the signal transducer. It is often the case that the readback signal is biased on a response curve that behaves nonlinearly with the amplitude of the input signal from the burst. Based on measurements made on Hewlett-Packard Cougar I disk drives with dual stripe MR heads, the distortion is primarily a quadratic term which adds zeroth and second harmonics to the readback signal

$$r(t) = R_0 (r_1 \sin \omega t + r_3 \sin 3\omega t + r_5 \sin 5\omega t + k_0 - k_0 \cos 2\omega t) + n(t). \quad (15)$$

(Note that other MR heads will most likely have different nonlinear distortions. Still, the notion of demodulating only harmonics that are advantageous holds. Only the specific choice of harmonics and their relative weighting changes.)

The matched filter equivalent for this signal would choose a mixing signal

$$m(t) = r_1 \sin \omega t + r_3 \sin 3\omega t + r_5 \sin 5\omega t + k_1 - k_1 \cos 2\omega t \quad (16)$$

which would maximize the demodulated signal with respect to the AWGN,  $n(t)$ , when  $k_0 = k_1$ . However this would also demodulate the terms caused by the nonlinear distortion which may result in a less useful signal for position sensing. In particular any change in the real time value of  $k_0$  (as might happen with changing track position or MR head bias current) would result in a large error. On the other hand, using the mixing signal defined in Equation 14 would completely avoid the terms which behave nonlinearly with burst amplitude. This is the type of flexibility that this algorithm gives us in building a servo demodulator.

### 3.3 Using Both Sine and Cosine Mixing Signals

We have discussed mainly mixing with a sum of sine waves because the particular shape of the dibit burst readback signal means that it is composed of sine waves. It should be apparent that if the readback signal takes a different shape, then a sum of cosine waves may also be used in

the mixing signal i.e.

$$m(t) = r_0 + \sum_{n=1}^{n_{max}} r_n \sin(n\omega t) + \sum_{k=1}^{k_{max}} s_k \cos(k\omega t). \quad (17)$$

Furthermore, if synchronization becomes an issue, we can mix with sine and cosine components separately and extract the amplitude of the burst signal using the square root of the sum of squares of the two individual (commonly called in phase and quadrature) results.

### 3.4 Implementation in Hardware

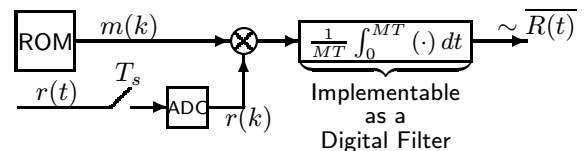


Figure 9: Digital circuit implementation of demodulator.

One function to mention here is the gating of the signals. Current technology for data channel demodulation should allow a clock recovery circuit to synchronize the mixing signal,  $m(t)$ , with the readback signal,  $r(t)$ . We assume that this has happened and that the residual jitter between the two signals is small enough to be considered negligible. Furthermore, the readback signal is gated so that the signal from the A Field is sent to the demodulator circuit for the A Field and the readback signal from the B Field is sent to the demodulator circuit for the B Field.

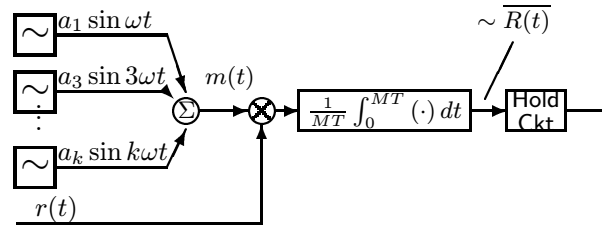


Figure 10: Analog circuit implementation of demodulator.

There are several options for implementing this in a chip. The choice of these turns out to be a tradeoff between the required speed of the circuitry and the simplicity of making adjustments to the mixing signal.

The simplest embodiment is the all digital implementation shown in Figure 9. In this case, the readback signal,  $r(t)$ , is sampled by an Analog to Digital Converter (ADC). The digital signal is then mixed with (multiplied by) samples of the mixing signal,  $m(k)$ , which have been read out of a Read Only Memory (ROM). This mixed signal is then integrated over the  $M$  periods of the dibit

for which the burst exists. This embodiment can probably be done on a single chip which contains the ADC, the ROM, and a signal processing element to do a numerical approximation of the integral. At the output, the data would already be in a digital form, so no further conversion would be needed. The main drawback to this embodiment is that the digital circuitry may not be fast enough to adequately demodulate the signals.

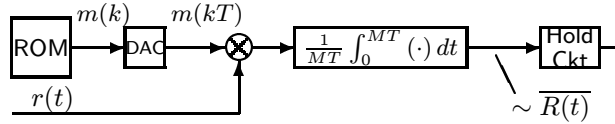


Figure 11: Hybrid analog/digital circuit implementation of demodulator.

At the other end of the spectrum is the all analog implementation shown in Figure 10. In this case, the mixing signal is generated as a weighted sum of  $n$  sine waves, each generated by its own oscillator circuit. However, as the number of oscillator circuits goes up, the complexity of this circuit rises. Furthermore, reprogramming the relative weights may be a problem.

In between these two methods is a hybrid analog/digital implementation shown in Figure 11. As with the digital implementation, a ROM is used to store the mixing signal, thus, the mixing signal may be adjusted and may have arbitrary complexity without changing the circuitry. The ROM outputs a sampled version of the mixing signal,  $m(k)$ , which is synchronized with the readback signal,  $r(t)$ . This signal is then passed through a Digital to Analog Converter (DAC) which produces a held continuous time analog version of the mixing signal,  $m(kT)$ . This signal is then mixed with (multiplied by) the readback signal,  $r(t)$ . This mixed signal is then integrated over the  $M$  periods of the dibit for which the burst exists. By sending the output of the ROM to a high speed DAC, the speed of the analog circuitry can be used in cases where circuit speed is an issue. The number of bits for the DAC should be chosen to keep the distortion due to quantization to an acceptably small level. Thus, this embodiment seems to maintain the best of both worlds.

## 4 Demodulation of Simulated and Real Data

The data shown below show the results of simulations comparing the rectify and integrate method of demodulation (often called area detection) with two different implementations of the new algorithm. One uses only the fundamental harmonic of the burst signal and thus is called ‘‘Sine Mixing.’’ The second case uses the first, third, and fifth harmonics of the burst in the same pro-

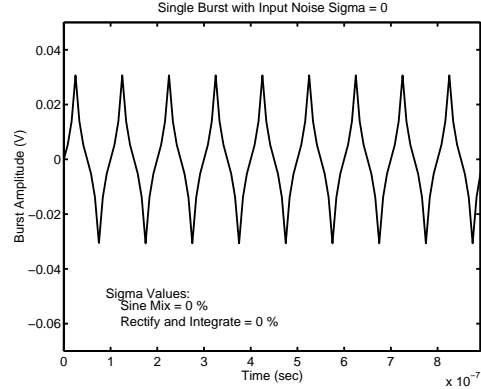


Figure 12: Ideal burst signal with no noise and no non-idealities.

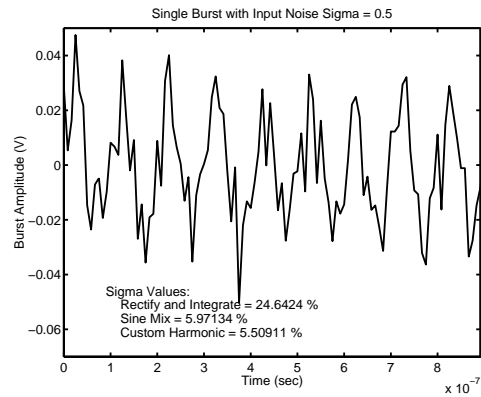


Figure 13: Single burst signal with additive noise. The standard deviation of the additive noise, ( $\sigma$ ), is given by  $\sigma = 0.5$ . The units are normalized so that amplitude of the fundamental frequency of the burst is 1. The entire burst is then scaled by a factor of 0.02 to better match the amplitude of bursts measured in the lab.

portions as they show up in the nominal noise free burst. This will be called the Custom Harmonic method. A third method which is analogous to the matched filter approach uses all the harmonics in the nominal burst. However, we can show how this can sometimes yield undesirable results and thus may not be as good as the Custom Harmonic method.

### 4.1 Computation of Error Measures

Some notes on how these numbers were computed are particularly useful. In general, the errors are normalized standard deviations. In our case, we normalize that standard deviation by the true mean of the number. In the case where we are generating a simulation, this true mean is the answer that one would get were there no noise or nonideality. This leads to the following relationship:

$$\sigma_{nor}(x) = \frac{E\{(x - \mu)^2\}^{\frac{1}{2}}}{\mu}. \quad (18)$$

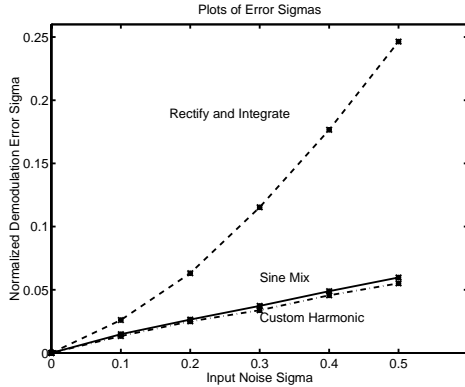


Figure 14: Comparison of standard deviations of sine mix and custom harmonic demodulation versus rectify and integrate demodulation schemes. The data was taken as the input noise on the burst was raised from  $\sigma = 0$  to  $\sigma = 0.5$  in the normalized units of the simulation.

In simulations, we know the true mean of the burst noise. In lab measurements the true mean can be estimated by averaging large numbers of measured bursts before estimating the mean. Given these “true means”, we approximate  $\sigma_{nor}$  via:

$$\sigma_{nor}(x) \approx \text{avg} \left| \frac{x_i - \mu}{\mu} \right|. \quad (19)$$

In this case, When a percentage is desired, the above number is multiplied by 100. We use the same notation when dealing with noise free nonidealities (Section 4.3). In this case  $\sigma_{nor}(x)$  represents a relative error, rather than a statistical quantity.

Note that computing a variance and a standard deviation from the true mean,  $\mu$ , is different from computing these quantities from the sampled mean. In particular, a rectifier will bias the AWGN leading to a nonzero sampled mean even when the true mean of the noise is 0.

## 4.2 Immunity to Broadband Noise

Figure 12 shows an ideal dibit burst and Figure 13 shows this burst with AWGN noise ( $\sigma = 0.5$ ) added to it. Both the Sine Mix and the Custom Harmonic demodulators have greater immunity to broadband noise than the rectify and integrate method. (Note that the rectify and integrate method has better noise immunity than a standard peak detection scheme[6].) In current drives a typical input noise level would correspond to the abscissa value of 0.1 on this plot. At this level, the new demodulator has roughly a factor of 2 improvement in noise immunity. However, it is important to note that as the input noise level goes up, the advantage of the new demodulator increases dramatically. This is shown clearly in Figure 14.

It is also worth noting that a square wave demodulator [10] – being composed entirely of odd harmonics – will not bias the noise and therefore should also perform better against AWGN than rectify and integrate. Generally speaking, however, demodulating harmonics at frequencies where there is little signal content but still some noise will lower the effective signal to noise ratio of the demodulation.

## 4.3 Adding Nonidealities to the Simulations

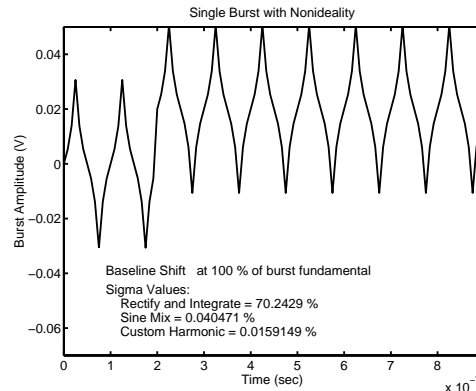


Figure 15: A noise free burst with a baseline shift starting at the third dibit.

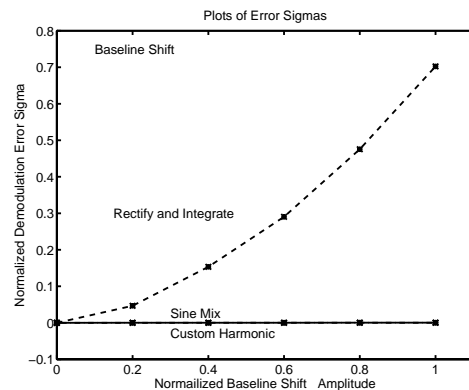


Figure 16: Comparison of standard deviations of sine mix and custom harmonic demodulation versus rectify and integrate demodulation schemes. The data was taken as the baseline shift starting at the third dibit was raised from 0 to 1.0 in the normalized units of the simulation.

This section addresses the addition of nonidealities. In order to have a common basis for comparison, several standards were maintained:

- A 9 dibit burst was always used to maintain consistency in the results and consistency with the disk drives from which measured data was obtained.

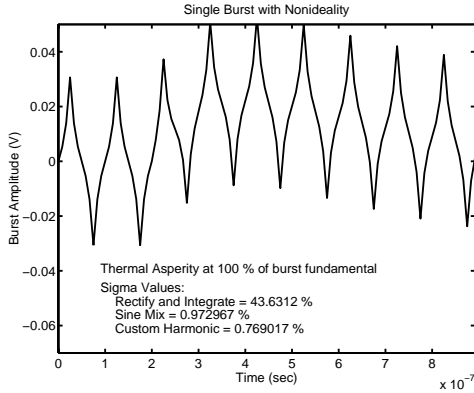


Figure 17: A noise free burst with a thermal asperity starting at the third dibit.

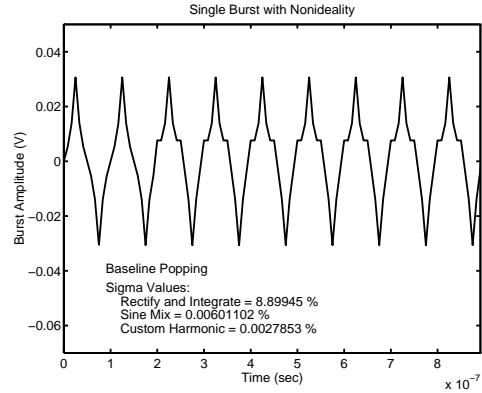


Figure 19: A noise free burst with baseline popping starting at the third dibit.

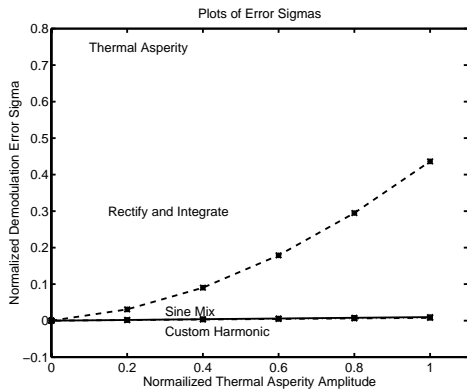


Figure 18: Comparison of standard deviations of sine mix and custom harmonic demodulation versus rectify and integrate demodulation schemes. The data was taken as the thermal asperity starting at the third dibit was raised from 0 to 1.0 in the normalized units of the simulation.

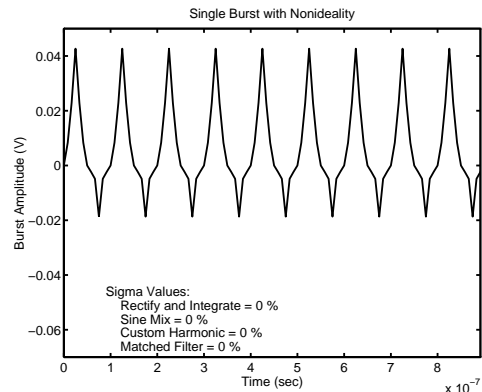


Figure 20: A noise free burst with a nominal second harmonic distortion scaled to 0.3 of the fundamental frequency amplitude.

- No random noise was added in simulations where the nonidealities were being added. While the real world has both of these phenomena, by thinking in the frequency domain about both the broadband noise and the nonidealities, we can see that it is possible to analyze them separately.
- The nonidealities always were started at the start of the 3rd dibit. This is for consistency and clarity of exposition. Such nonidealities as baseline shift would be less obvious if they were started at the first dibit.
- The nonidealities were scaled relative to the amplitude of the fundamental frequency of the servo burst. Thus, a scale of 1 implies that the fundamental frequency of the servo burst has the same amplitude as the nonideality. The burst itself – being comprised of several harmonics – may have higher amplitude.

#### 4.3.1 Drop In and Drop Out

A Drop In will be defined in this paper as a sudden increase in amplitude of a single burst bit. Likewise, a Drop Out is a sudden absence of a single burst bit. As both of these happen at the fundamental frequency of the burst, the new algorithm can do nothing to select it out. Neither of these are improved or made worse by the demodulation algorithm. Results are omitted for the sake of brevity.

#### 4.3.2 Baseline Shift

Baseline Shift is a sudden increase in the offset of the burst. This is shown in Figures 15 and 16. It creates a large effect on the rectify and integrate demodulator, but virtually none on the new demodulator.

#### 4.3.3 Thermal Asperity

A Thermal Asperity causes a rapid increase and then gradual decrease in the response from the head. This is shown in Figures 17 and 18. It creates a large effect on

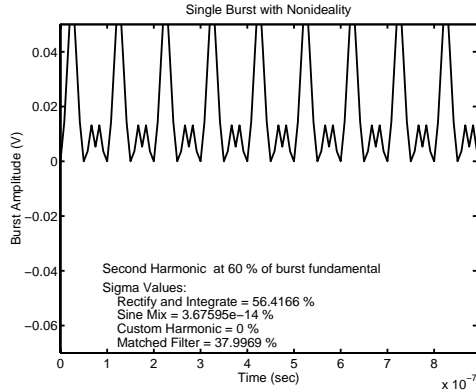


Figure 21: A noise free burst with a nominal second harmonic distortion scaled to 0.3 of the fundamental frequency amplitude. An additional second harmonic distortion term of 0.6 of the fundamental frequency amplitude is added in.

the rectify and integrate demodulator, but virtually none on the new demodulator.

#### 4.3.4 Baseline Popping

With Baseline Popping, the nominal quiescent value of the a dibit pulse returns to a nonzero value. This is shown in Figure 19. This causes some problems for the rectify and integrate detector, but none for the new demodulator. Unfortunately, this does not lend itself well to being plotted in the sigma value plots, so only one example is given.

#### 4.3.5 Second Harmonic Distortion

The Second Harmonic Distortion discussed earlier is shown in Figure 20. It results in an asymmetric pulse shape. When the amount of second harmonic distortion deviates from the nominal level as shown in Figure 21, then both the rectify and integrate and matched filter methods exhibit dramatic error levels. This is due to the fact that since the matched filter demodulates frequencies that include the second harmonic distortion it demodulates the erroneous component as well, causing an error. Note also that since neither the Sine Mix nor the Custom Harmonic schemes demodulate these frequencies, they are immune to any second harmonic distortion as shown in Figure 22. A square wave demodulation method, being composed only of odd harmonics (Section 3.1), is also immune to distortion in the second (or any even) harmonic. (However, in the case of an MR head, if the distortion occurs in some odd harmonic, then a square wave demodulation algorithm would be susceptible, while a Custom Harmonic algorithm could be designed to avoid those harmonics.)

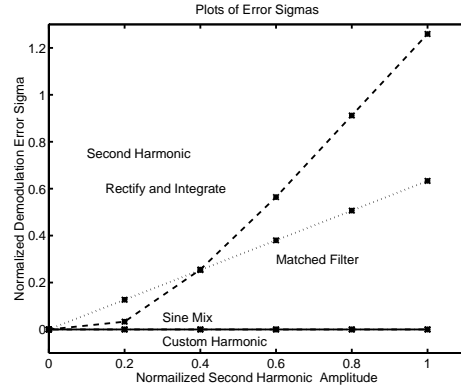


Figure 22: Comparison of standard deviations of sine mix, custom harmonic, and matched filter demodulation versus rectify and integrate demodulation schemes. To the noise free burst with the nominal second harmonic distortion scaled to 0.3 of the fundamental frequency amplitude was added additional second harmonic distortion terms scaled from 0 to 1.0 of the fundamental frequency amplitude is added in.

## 5 Discussion

Note that in all cases the Sine Mix demodulator and the Custom Harmonic demodulator provide dramatic improvement over standard rectify and integrate. The Custom Harmonic demodulator also always does better than the Sine Mix demodulator, but the difference is small. The choice of Custom Harmonic versus Sine Mix is really one of slightly improved noise immunity versus potentially greater complexity. Note, though, that two of the implementation methods simply store the mixing signal in ROM and thus there is no added complexity in implementing the Custom Harmonic version over the Sine Mix version. The improved noise immunity is essentially free.

Note that the Custom Harmonic method also gives more freedom to avoid such MR head phenomena as second harmonic distortion. What this means is that for the cost of some extra silicon in the servo demodulator, we can achieve dramatically improved immunity to both broadband noise and certain transducer phenomena that currently plague conventional servo demodulators. Furthermore, by removing the susceptibility to distortions in certain harmonics, the fact that the MR head produces an asymmetric pulse shape is irrelevant. The servo channel will only see the symmetric portion of the signal. This can save us the trouble of attempting to remove this asymmetry in other ways – such as creating a dual stripe MR head or a dual stripe Giant Magneto-Resistive (GMR) or Colossal Magneto-Resistive (CMR) head. In particular, process variations can leave residual asymmetries in such heads. Of course, servo signals demodulated from these heads these heads can have their responses linearized by use of the Sine Mix or Custom Harmonic demodulators.

## References

- [1] R. C. Blackham, J. A. Vasil, E. S. Atkinson, and R. W. Potter, "Measurement modes and digital demodulation for a low-frequency analyzer," *Hewlett-Packard Journal*, vol. 38, pp. 17–25, January 1987.
- [2] D. Abramovitch, T. Hurst, and D. Henze, "The PES Pareto Method: Uncovering the strata of position error signals in disk drives," in *Proceedings of the 1997 American Control Conference*, (Albuquerque, NM), AACC, IEEE, June 1997.
- [3] T. Hurst, D. Abramovitch, and D. Henze, "Measurements for the PES Pareto Method of identifying contributors to disk drive servo system errors," in *Proceedings of the 1997 American Control Conference*, (Albuquerque, NM), AACC, IEEE, June 1997.
- [4] D. Abramovitch, T. Hurst, and D. Henze, "Decomposition of baseline noise sources in hard disk position error signals using the PES Pareto Method," in *Proceedings of the 1997 American Control Conference*, (Albuquerque, NM), AACC, IEEE, June 1997.
- [5] D. Abramovitch, T. Hurst, and D. Henze, "An overview of the PES Pareto Method for decomposing baseline noise sources in hard disk position error signals," To appear in the *IEEE Transactions on Magnetics*, January 1998.
- [6] Silicon Systems, *Integrated Circuits for Storage Products*, 1995.
- [7] Z.-E. Boutaghou, D. H. Brown, K. J. Erickson, and R. Greenberg, "Digital servo signal demodulation method and apparatus utilizing a partial-response maximum-likelihood (prml) channel in a disk file," United States Patent 5,343,340, International Business Machines Corporation, Armonk, NY USA, August 1994.
- [8] H. Yada and T. Takeda, "A Coherent Maximum Likelihood Head Position Estimator for PERM Disk Drives," *IEEE Transactions on Magnetics*, May 1996.
- [9] J. M. Mendel, *Lessons in Digital Estimation Theory*. Englewood Cliffs, NJ: Prentice-Hall, 1987.
- [10] R. S. Wilson, "Sample data position error signal detection for digital sector servo," United States Patent 5,301,072, Mastor Corporation, San Jose, CA USA, April 1994.